



## Antibacterial Evaluation, *In Silico* Study and ADMET Properties of Local *Lawsonia inermis* Leaves Extract

Zainab R. Abdulhussein<sup>1</sup>, Munther A. Muhammad-Ali<sup>2,\*</sup>, Ekhlas Q. Jasim<sup>1</sup><sup>1</sup>Department of Pathological Analyses, College of Science, University of Basrah, Basrah, Iraq<sup>2</sup>Department of Ecology, College of Science, University of Basrah, Basrah, Iraq**ARTICLE INFO****ABSTRACT****Article history:**

Received 24 January 2025

Revised 21 February 2025

Accepted 12 March 2025

Published online 01 May 2025

**Copyright:** © 2025 Abdulhussein *et al.* This is an open-access article distributed under the terms of the [Creative Commons Attribution License](https://creativecommons.org/licenses/by/4.0/), which permits unrestricted use, distribution, and reproduction in any medium, provided the original author and source are credited.

Plant extracts are important in the treatment of many bacterial infections, including henna extracts. Pharmacognosy have become an alternative to traditional medications because of a synergistic effect in combating bacterial infections and no multiple side effects. This investigation examined the antibacterial efficacy of *Lawsonia inermis* acetone extract against bacteria isolated from urinary tract infections (UTIs) and wounds, including *Pseudomonas aeruginosa*, *Staphylococcus aureus*, *Klebsiella pneumoniae*, and *Escherichia coli*. To isolate the pathogenic bacteria (*P. aeruginosa*, *S. aureus*, *K. pneumoniae*, and *E. coli*), clinical pathogenic samples were obtained. Acetone extract of *Lawsonia inermis* leaves was produced using Soxhlet extraction and the solution of solid extract was investigated by the cork borer technique which gave an inhibitory zone of 18 to 22 mm against the four species of bacteria. 16 phytochemicals (*Ia-Ip*) were identified in the extract using gas chromatography-mass spectrophotometry (GC-MS) peak area percentage (10.66-1.72%). The analysis of phytochemicals using molecular docking simulations of their antibacterial potential revealed binding affinities of -4.38 to -7.83 kcal/mol, -4.67 to -7.47 kcal/mol, -5.06 to -9.07 and -4.41 to -7.30 kcal/mol against the dihydropteroate synthase and gyrase B 24kDa proteins of *E. coli*, and TyrRS and gyrase B proteins of *S. aureus*, respectively. The extract phytochemicals were subjected to physicochemical parameters evaluation: ADMET predictions. Pharmacokinetic prediction indicates fewer adverse effects. The extract has potential antimicrobial activity, with higher levels of clinical safety based on ADMET predictions.

**Keywords:** Henna plant, Molecular docking, Antibacterial activity, Phytochemicals, pharmacokinetic properties

**Introduction**

Biologically active, naturally occurring chemical compounds found in plants, called phytochemicals (from the Greek word phyto, meaning plant) have health advantages for humans beyond those associated with macronutrients and micronutrients.<sup>1</sup> They enhance the colour, flavour, and perfume of plants while shielding them from harm and disease. Generally speaking, phytochemicals are the plant compounds that shield plant cells from environmental dangers like pollution, stress, dehydration, ultraviolet exposure, and pathogenic attack.<sup>2,3</sup> In recent times, it has been evident that they play a part in safeguarding human health when they consume large amounts of food. Almost 4,000 phytochemicals have been categorized and arranged according to their chemical makeup, physical attributes, and protective roles.<sup>4,5</sup> During that time, the use of medicinal plants has nearly doubled in Asia. The main causes of this resurgence of interest include ecological consciousness, the effectiveness of many phytopharmaceutical preparations, such as ginkgo, garlic, or valerian, and the growing interest of large pharmaceutical corporations in higher medicinal plants.<sup>6</sup>

\*Corresponding author. E mail: [munther.ali@uobasrah.edu.iq](mailto:munther.ali@uobasrah.edu.iq)

Tel.: +9647705615571

**Citation:** Abdulhussein ZR, Muhammad-Ali MA, Jasim EQ. Antibacterial Evaluation, *In Silico* Study and ADMET Properties of Local *Lawsonia inermis* Leaves Extract. Trop J Nat Prod Res. 2025; 9(4): 1599 – 1609 <https://doi.org/10.26538/tjnpr/v9i4.32>

Official Journal of Natural Product Research Group, Faculty of Pharmacy, University of Benin, Benin City, Nigeria

Frequent consumption of nutrient-dense foods (rich in phytochemicals) has been linked to several health benefits, including protection against acute and chronic metabolic or degenerative diseases such as diabetes, cancer, cardiovascular disease, and neurodegenerative diseases like Parkinson's, Alzheimer's, and others.<sup>7,8</sup> Phytoconstituents function as cofactors, substrates, and inhibitors of enzymatic and biochemical reactions to produce their effects, as ligands, they are employed as agonists or antagonists at intracellular receptors on the cell surface and as scavengers of harmful substances. As chelates, they bind and eliminate undesirable components in the Gastrointestinal tract (GIT).<sup>9</sup> They are utilized as components that increase the stability and absorption of certain essential nutrients in addition to serving as essential development factors.<sup>10</sup>

The henna plant (*Lawsonia inermis* L.) is indigenous to the Indian subcontinent, the Middle East, and North Africa. For thousands of years, people in North Africa and Asia have used henna, a plant that blooms in sunny climates, as a red dye and perfume. Mummies in ancient Egypt were covered in textiles stained with henna. *Lawsonia inermis* L. has demonstrated antimicrobial, antifungal<sup>11</sup>, antitumor<sup>12</sup>, larvicidal, antileishmanial, antimalarial<sup>13</sup>, hepatoprotective and antioxidant<sup>14</sup>, wound healing<sup>15</sup>, anti-inflammatory, analgesic, antipyretic<sup>16</sup>, memory enhancement<sup>17</sup>, and enzyme inhibitor<sup>18</sup> properties in pharmacological studies.

Iraq is home to several henna species that are cultivated around the southern region of Iraq, particularly around Faw ([29.999289, 48.440181](https://doi.org/10.26538/tjnpr/v9i4.32)), Basrah Governorate, Iraqi henna is widely used<sup>19</sup>. This study's two main goals were to: (1) investigate the *Lawsonia inermis* acetone extract's potential for *in vitro* antibacterial action against *Escherichia coli* (*E. coli*) and *Staphylococcus aureus* (*S. aureus*); and

(2) predict potential compounds identified by Gas Chromatography-Mass Spectrometry (GC-MS) using *in silico* analysis, binding interactions via molecular docking, and Absorption, Distribution, Metabolism, and Excretion-Toxicity (ADMET) pharmacokinetic characteristics.

## Materials and Methods

### Materials and instruments

Acetone (99.94%, Sigma), Dimethyl sulphoxide (DMSO) (99.5%, HiMedia, India), Ferric chloride (99.74%, Aldrich), Hydrochloric acid (37.35%, Sigma), Muller-Hinton and Nutrient agar (HiMedia, India), Incubator and Mini vortex (Fisher Scientific, USA), Centrifuge (Model PLC-012, Gemmy Instrument Corp., Taiwan).

### Collection and diversity of plant materials

*Lawsonia inermis* leaves (VN310, BSRA) were collected in the neighbourhood of Basra (30.499036, 47.847679), Iraq, in September 2023. The plant was chopped into tiny pieces, cleansed in distilled or tap water, and then let air dry in the shade at room temperature. An electric grinder was used to ground the leaves into a fine powder. The powdered plant sample was extracted with Acetone using the Soxhlet apparatus. After, 48 hours the extract was concentrated in a rotary evaporator to obtain a crude extract with a volume of approximately 20 mL. The extract was then allowed to dry at room temperature.

### Antibacterial Test

Antibacterial activity was determined by distributing 20 µL of the available pathogenic cultures across nutrient agar plates using Kirby Bauer's agar well diffusion method. Wells with a 7 mm diameter were drilled using a sterile borer. To function as a control, the extract was also added into the wells along with DMSO. Antibiotics were used at a dosage of 1000 µg/mL with standard disc diffusion. Using an agar well diffusion test, the antibacterial activity of *Lawsonia inermis* extract against *Pseudomonas aeruginosa*, *Staphylococcus aureus*, *Klebsiella pneumoniae*, and *Escherichia coli* isolated from UTI and wound infection were assessed at dosages of 1000 and 500 µg/mL. Every plate was then incubated for 24 hours at 37°C. The inhibition zone was measured in millimetres to assess the extract's antibacterial effectiveness against two different bacterial strains.<sup>20</sup>

### Primarily Phytochemical Screening

The phytochemical components of *Lawsonia inermis* leaf extract were identified using conventional extraction and screening techniques.

### Tannins Test

To determine the tannin, 500 mg of the *Lawsonia inermis* leaf crude extract was filtered and combined with 10 mL of distilled water. FeCl<sub>3</sub> was added to the filtrate to produce a blue, blue-black, green, or blue-green hue to confirm the presence of tannin.<sup>21</sup>

**Flavonoids Test:** Shinoda test: A few pink scarlets, crimson red, or occasionally green to blue colour appearances emerged that were considered to indicate the presence of flavonoids when a little amount of magnesium was added to the extract, followed by the dropwise addition of concentrated hydrochloric acid.<sup>22</sup>

### Phenolic Compounds Test

**FeCl<sub>3</sub> Test:** To 1 mL of the filtered plant extract sample, a few drops of a 10% ferric chloride solution were added. The development of green, blue, or violet colour indicates the existence of phenolic chemicals.<sup>23</sup>

### Saponins Test

In a test tube, 500 mg of the crude extract was shaken with water to confirm the presence of saponins. The creation of froth that held up to heating was proof that saponin was present.<sup>24</sup>

### GC-MS Analysis

The Perkin-Elmer Clarus 680 system (Perkin-Elmer, Inc., U.S.A.) was used for GC-MS analysis of leaf extracts. It had a fused silica column

(30 m in length, 250 µm in diameter, and 0.25 µm in thickness) filled with Elite-5MS capillary columns. The carrier gas, which was 99.99 percent pure, was pumped at a constant rate of 1 mL per minute. An electron ionization energy technique was employed for GC-MS spectrum detection, with a high ionization energy of 70 eV (electron Volts), a scan length of 0.2 s, and fragments ranging from 40 to 600 m/z. The injector temperature was kept at 250 °C while one litre of injection was made at a split ratio of 10:1. Initially, 50 °C was set as the column oven's temperature for three minutes. It was then elevated to 280 °C by 10 °C per minute until it was at 300 °C for ten minutes. The mass, peak area, peak height, and retention time (min) spectrum patterns of the samples were compared with spectral databases of genuine compounds kept in the National Institute of Standards and Technology (NIST) library to determine which phytochemicals were present.

### In Silico Analyses of the phytochemicals

#### Ligand and Target Protein Preparation, and Molecular Docking

The ChemOffice application (Chem sketch 16.0) was used to sketch the chemical structures of phytochemicals with the appropriate 2D orientation. With the aid of molecular docking and MOE 2022 v2 software (Chemical Computing Group, France), all ligand and water molecules were eliminated from the isolated compounds. The crystal structures of *E. coli* [Dihydropteroate Synthase (protein ID: 1AJ0), Gyrase B 24kDa (protein ID: 6F86)] and *S. aureus* [TyrRS (protein ID: 1JJJ), Gyrase B (protein ID: 3G75)] were obtained from the RCSB protein data database. The Protein Data Bank (PDB), accessible at (<https://www.rcsb.org/>), provided the protein data for all of the samples.<sup>25,26</sup>

#### ADMET Profiling of the phytochemicals

For *in silico* prediction, the simplified molecular-input line-entry system (SMILES) forms for every compound were used from ChemDraw 16.0. The ADMETlab 2.0 web server (<http://www.admetmesh.scbdd.com/>) was the platform for the physicochemical analysis (accessed on August 15, 2024). The pkCSM web server (<https://biosig.lab.uq.edu.au/pkcsml/>) was used to run analyses of the pharmacokinetic features (absorption, distribution, metabolism, excretion, and toxicity) (accessed on 15 Aug 2024).<sup>27,28</sup>

## Results and Discussion

The phytochemical screening of the acetone extract of *Lawsonia inermis* leaves showed the presence of flavonoids, tannins, phenols, and saponins. The pH of the extract was 5.3.

The GC-MS analysis of *Lawsonia inermis* extracts in acetone produced a GC-MS chromatogram with 58 peaks. These peaks were determined to be the bioactive compounds by comparing their mass spectral fragmentation patterns, peak retention times, peak areas (percent), and peak heights (percent) to those of the well-known compounds in the NIST library. Table 1 and Figure 1 show the GC-MS results of the first sixteen compounds (*1a-1p*) with decreasing sort of peak area percentage (10.66-1.72%). In another study, the isolation showed that there are many bioactive compounds such as lactones<sup>29</sup> with good concentrations such as *1a*, *1b*, *1c*, *1d*, *1h* and *1o*, *1j* (vitamin E), *1g*, *1l* (fatty acids), *1n* (piperine) and *1f* (naphthoquinone). The following are the major phytoconstituents with high concentrations and their peak area percentages: (3,6,9-Trimethylidene-2-oxo-3a,4,5,6a,7,8,9a,9b-octahydroazuleno[4,5-b]furan-8-yl) acetate (10.66%), Dehydrocostus lactone (9.18%), Reynosin (7.35%), Azuleno[4,5-b]furan-2(3H)-one, 3a,4,6a,7,8,9,9a,9b-octahydro-6-methyl-3,9-bis(methylene)-, [3aS-(3a.alpha.,6a.alpha.,9a.alpha.,9b.beta.)]- (7.03%), Tricyclo[6.3.3.0]tetradec-4-ene,10,13-dioxo- (5.80%), and 6,7-Dimethyl-5-nitro-1,4-naphthoquinone (5.79%).

In a previous study, ethanolic and aqueous *Lawsonia inermis* showed effective antibacterial activity against Gram-positive and Gram-negative bacteria such as *Staphylococcus xylosus*, *Serratia ficaria*, *klebsiella oxytoca* and *Escherichia coli*<sup>30</sup>, which is in line with the current study. Similar results were reported by another study that concluded the antibacterial activity of ethanolic *Lawsonia inermis* extract against *Aggregatibacter*

*actinomycetemcomitans* and *Porphyromonas gingivalis* bacteria.<sup>31</sup> Acetone extract of *Lawsonia inermis* leaf (1000 µg/mL) gave antibacterial activity against the studied bacteria with an inhibition zone of 20, 20, 18, and 22 mm for *E. coli*, *K. pneumoniae*, *P. aeruginosa*, and *S. aureus*, respectively, as shown in Figure 2. These antibacterial properties of the plant extracts are due to the presence of enriched

constituents like polyphenols, flavonoids, and tannins.<sup>32</sup> The higher contents of lactones in the plant extracts were detected in the current study which act as antibacterial agents.<sup>33</sup> The phytochemical compounds detected by GC-MS analysis classified as lactones, phenols, fatty acids, and quinones, as shown in Figure 1, have been proven to express antibacterial potency against many types of bacteria.<sup>34,35</sup>

**Table 1:** Phytochemical compounds identified in acetone *Lawsonia inermis* leaf extract using GC-MS

No.	Name of the compound	Molecular formula	Molecular weight	Peak area (%)	RT (min)
1a	(3,6,9-Trimethylidene-2-oxo-3a,4,5,6a,7,8,9a,9b-octahydroazuleno[4,5-b]furan-8-yl) acetate	C <sub>17</sub> H <sub>20</sub> O <sub>4</sub>	288.34	10.66	25.84
1b	Dehydrocostus lactone	C <sub>15</sub> H <sub>18</sub> O <sub>2</sub>	230.31	9.18	23.10
1c	Reynosin	C <sub>15</sub> H <sub>20</sub> O <sub>3</sub>	248.32	7.35	25.17
1d	(3aS,6aR,9aR,9bS)-6-methyl-3,9-dimethylene-3a,4,6a,7,8,9,9a,9b-octahydroazuleno[4,5-b]furan-2(3H)-one	C <sub>15</sub> H <sub>18</sub> O <sub>2</sub>	230.31	7.03	23.20
1e	(Z)-4,5,8,9-tetrahydro-1H-3a,9a-propanocyclopenta[8]annulene-2,11(3H)-dione	C <sub>14</sub> H <sub>18</sub> O <sub>2</sub>	218.30	5.80	24.99
1f	6,7-Dimethyl-5-nitro-1,4-naphthoquinone	C <sub>12</sub> H <sub>9</sub> NO <sub>4</sub>	231.21	5.79	27.06
1g	n-Hexadecanoic acid	C <sub>16</sub> H <sub>32</sub> O <sub>2</sub>	256.43	4.18	22.66
1h	Santamarine	C <sub>15</sub> H <sub>20</sub> O <sub>3</sub>	248.32	4.09	24.86
1i	gamma-Sitosterol	C <sub>29</sub> H <sub>50</sub> O	414.72	3.41	34.08
1j	Vitamin E	C <sub>29</sub> H <sub>50</sub> O <sub>2</sub>	430.72	2.89	32.10
1k	2,4,6-Triisopropylbenzoyl chloride	C <sub>16</sub> H <sub>23</sub> ClO	266.81	2.61	26.75
1l	Oleic Acid	C <sub>18</sub> H <sub>34</sub> O <sub>2</sub>	282.47	2.26	24.34
1m	Neophytadiene	C <sub>20</sub> H <sub>38</sub>	278.52	2.03	21.37
1n	Piperine	C <sub>17</sub> H <sub>19</sub> NO <sub>3</sub>	285.34	1.97	30.53
1o	Spirafolide	C <sub>15</sub> H <sub>18</sub> O <sub>3</sub>	246.31	1.82	22.85
1p	Celestolide	C <sub>17</sub> H <sub>24</sub> O	244.38	1.73	25.34

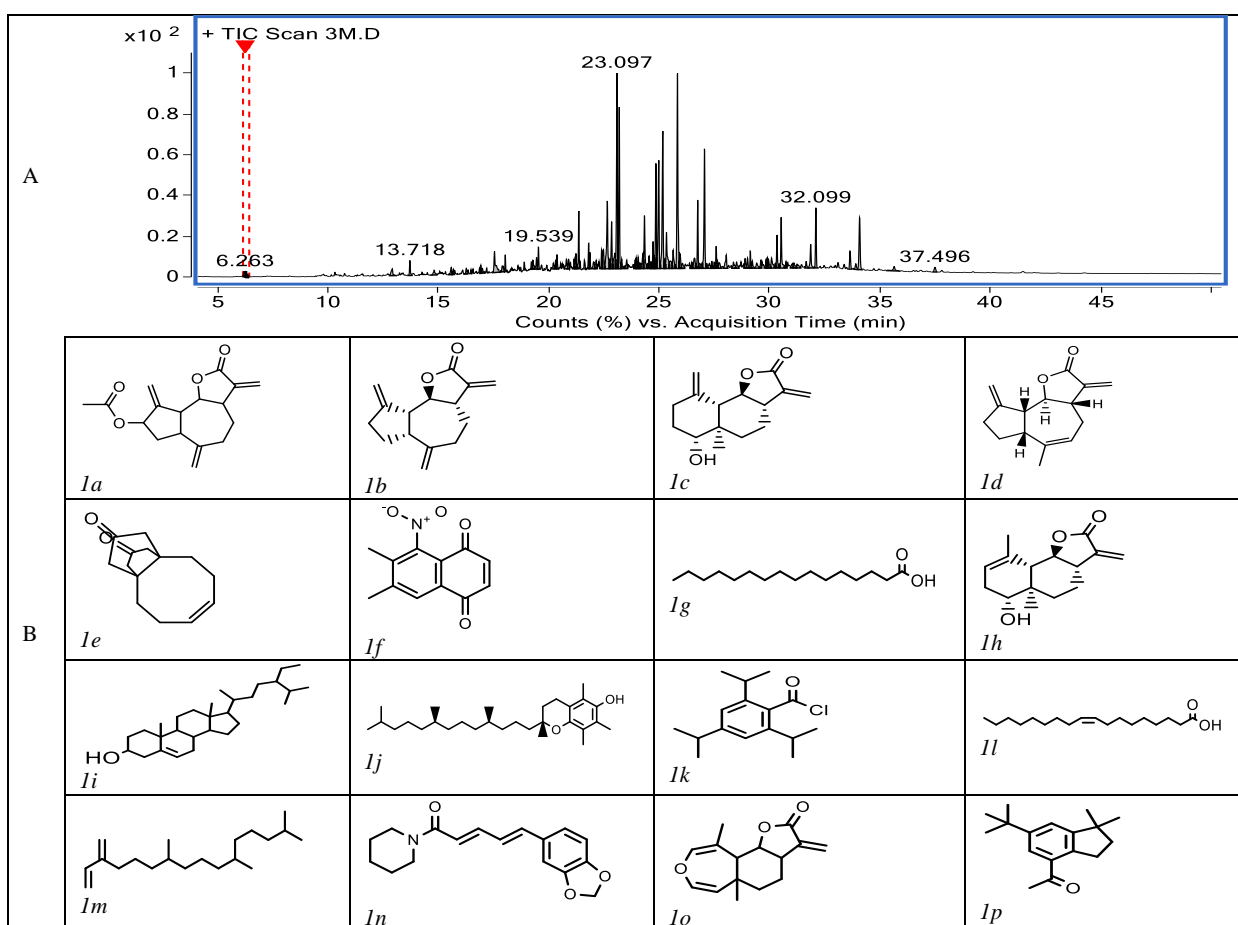


**Figure 1:** (A) GC-MS chromatogram of *Lawsonia inermis* leaf extract. (B) Chemical structures of the phytochemicals

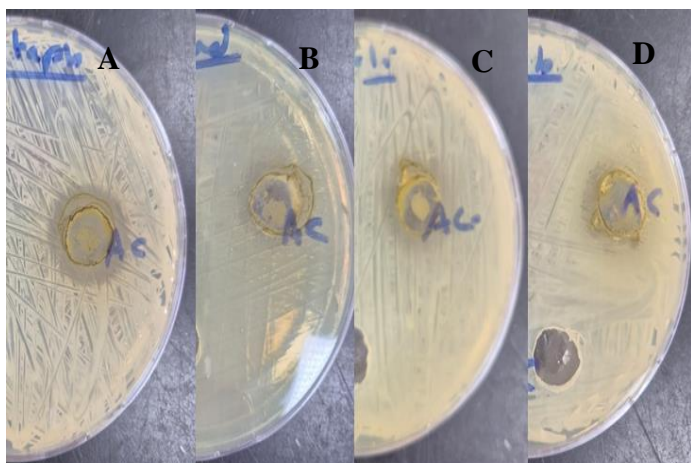


**Figure 2:** The antibacterial activity of the 1000 µg/mL extract against *S. aureus* (A), *P. aeruginosa* (B), *E. coli* (C), and *K. pneumoniae* (D)

In the current study, the phytochemical compounds (*Ia–Ip*) were subjected to a molecular docking analysis to examine their interaction pattern with dihydropteroate synthase (1AJ0 protein) and DNA gyrase B (6F86 protein) of *E. coli*. Table 2 shows that the sixteen compounds had minimum binding energies ranging from  $-4.38$  to  $-7.83$  kcal/mol against dihydropteroate synthase. Compounds *Ig*, *Ii*, *Ij*, and *Ih* among the docked compounds had a high S-score ( $-7.05$ ,  $-7.18$ ,  $-7.83$ , and  $-7.26$  kcal/mol, respectively) in comparison to the conventional medication ceftriaxone ( $-7.21$  kcal/mol). Compound *Ig* formed Van der Waals connections with HIS257 and has hydrogen bonds with LYS221 and ARG255, it also has ionic interactions with LYS221 and ARG255 (Table 3 and Figure 3). However, as Table 3 and Figure 4 demonstrate, compound *Ih* also has an ionic contact with LYS221 and GLY217 as well as an H-bond with LYS221 with dihydropteroate synthase. Similarly, the sixteen compounds' interactions with the *E. coli* DNA gyrase B were evaluated. Minimum binding energy was found using docking research to range from  $-4.67$  to  $-7.47$  kcal/mol (Table 2). When compared to the conventional ceftriaxone ( $-6.66$  kcal/mol), the docked compounds *Ig* and *Ih* had a better interaction with the same protein ( $-7.45$  and  $-7.47$  kcal/mol, respectively). Table 3 and Figures 5 and 6 highlight the H bonds and ionic interactions that these two compounds demonstrated with ARG136 and ARG76

**Table 2:** Docking scores of conventional pharmaceuticals and phytochemical compounds covalently linked to the active site of *E. coli* dihydropteroate synthase (protein ID: 1AJ0), *E. coli* DNA Gyrase B 24kDa (protein ID: 6F86), *S. aureus* TyrRS (protein ID: 1J1J), and *S. aureus* DNA gyrase B (protein ID: 3G75).

Compd.	1AJ0			6F86			1J1J			3G75		
	S Score (kcal/mol)	RMSD (Å)		S Score (kcal/mol)	RMSD (Å)		S Score (kcal/mol)	RMSD (Å)		S Score (kcal/mol)	RMSD (Å)	
<i>Ia</i>	-5.85	2.33		-5.86	2.58		-6.54	2.56		-5.95	1.85	
<i>Ib</i>	-5.11	1.47		-5.26	2.66		-5.83	0.84		-5.19	1.03	
<i>Ic</i>	-4.91	1.58		-5.53	0.85		-5.06	1.78		-5.01	2.13	
<i>Id</i>	-5.09	0.97		-5.39	2.13		-6.14	1.04		-5.42	1.12	
<i>Ie</i>	-4.38	1.78		-4.72	1.87		-5.21	1.95		-4.41	2.05	
<i>If</i>	-5.29	1.29		-5.00	2.30		-6.09	1.89		-5.63	1.21	
<i>Ig</i>	-7.05	1.49		-7.45	1.87		-7.21	1.74		-6.86	2.32	
<i>Ih</i>	-5.18	2.22		-5.11	1.83		-5.48	2.56		-4.96	2.36	
<i>Ii</i>	-7.18	1.55		-6.02	2.27		-7.41	2.70		-5.62	2.11	
<i>Ij</i>	-7.83	1.56		-6.77	2.11		-9.07	2.17		-7.30	1.90	
<i>Ik</i>	-5.55	2.43		-4.67	2.25		-6.64	1.94		-5.75	2.56	
<i>Il</i>	-7.26	1.78		-7.47	1.32		-7.94	2.02		-7.27	1.63	
<i>Im</i>	-6.26	1.67		-6.03	2.14		-7.82	2.06		-6.51	1.96	
<i>In</i>	-6.60	1.42		-5.92	1.49		-6.87	1.50		-6.28	0.86	
<i>Io</i>	-4.60	1.41		-5.13	2.15		-5.19	1.31		-4.56	2.25	
<i>Ip</i>	-5.41	0.85		-4.99	1.61		-6.97	1.46		-5.49	1.38	
Ceftriaxone	-7.21	1.85		-6.66	2.14		-9.53	1.47		-7.54	2.01	

**Table 3:** Molecular docking data of phytochemicals against *E. coli* proteins

Compd	1AJ0 protein				6F86 protein				
	Ligand–Amino acid Interaction	Types of Interactions	Distance (Å)	Interaction Energy (kcal/mol)	Ligand–Amino acid Interaction	Types of Interactions	Distance (Å)	Interaction Energy (kcal/mol)	
<i>Ia</i>	O32 – ARG235	H-acceptor	3.41	-28.19	O6 – ARG76	H-acceptor	3.17	-30.83	
<i>Ib</i>	O31 – ARG235	H-acceptor	3.43	-21.29	O31 – ASN46	H-acceptor	3.37	-24.85	
<i>Ic</i>	O30 – ARG235	H-acceptor	3.15	-14.87	O34 – ARG136	H-acceptor	3.23	-25.40	
<i>Id</i>	O21 – ARG235	H-acceptor	3.30	-15.37	O21 – ARG136	H-acceptor	3.26	-25.08	
<i>Ie</i>				-12.37				-20.57	
<i>If</i>	O15 – ARG235	H-acceptor	3.03	-21.02	O15 – ASN46	H-acceptor	3.37	-24.69	
	6-ring – SER222	pi-H	4.25		O17 – ARG76	H-acceptor	2.99		
					6-ring – GLU50	pi-H	3.86		
<i>Ig</i>	O48 – LYS221	H-acceptor	3.08	-31.71	O48 – ARG136	H-acceptor	3.27	-33.98	
	O49 – ARG255	H-acceptor	3.26		O49 – ARG136	H-acceptor	2.94		
	O48 – LYS221	Ionic	3.08		O48 – ARG76	Ionic	3.10		

	O49 – ARG255	Ionic	3.26		O48 – ARG136	Ionic	3.27	
	C44 – HIS257	H-pi	4.28		O49 – ARG136	Ionic	3.20	
<i>Ih</i>	O37 – ARG63	H-acceptor	2.86	-22.52	O31 – ASN46	H-acceptor	3.26	-24.82
<i>Ii</i>				-15.54				-30.31
<i>Ij</i>				-14.63	O80 – GLY77	H-donor	2.86	-37.39
					6-ring – ARG76	pi-cation	3.21	
<i>Ik</i>	O10 – ARG235	H-acceptor	3.30	-23.58	O10 – ARG76	H-acceptor	3.26	-19.41
	6-ring – SER222	pi-H	4.07					
<i>Il</i>	O52 – LYS221	H-acceptor	3.10	-26.98	O52 – ARG76	H-acceptor	3.04	-32.76
	O53 – GLY217	H-acceptor	3.35		O53 – ARG136	H-acceptor	3.02	
	O52 – LYS221	Ionic	3.10		O52 – ARG76	Ionic	3.04	
					O53 – ARG136	Ionic	2.96	
<i>Im</i>				-26.44				-20.40
<i>In</i>	C23 – MET139	H-donor	3.96	-25.92	O20 – ARG136	H-acceptor	3.32	-32.59
					O20 – ARG136	H-acceptor	3.00	
					6-ring – ILE78	pi-H	3.90	
<i>Io</i>	O31 – SER222	H-acceptor	2.79	-18.41				-25.73
<i>Ip</i>	O38 – ARG235	H-acceptor	3.27	-23.21	O38 – ARG136	H-acceptor	3.15	-23.98

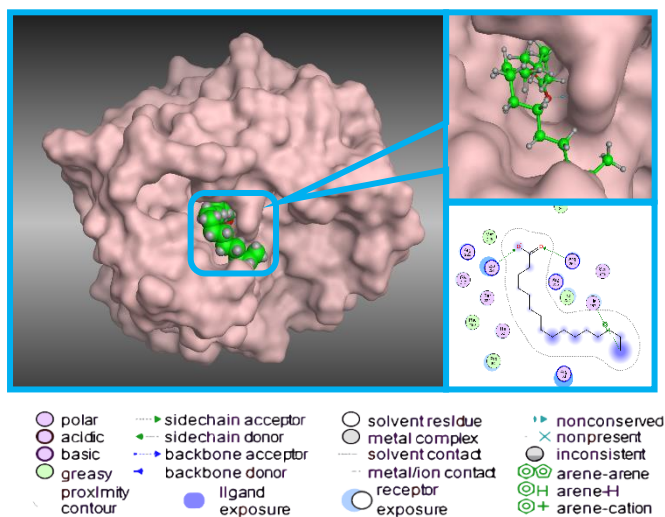


**Figure 3:** (a) Surface and (b) 2D view of docked conformation of *Ig* against *E. coli* 1AJ0 protein

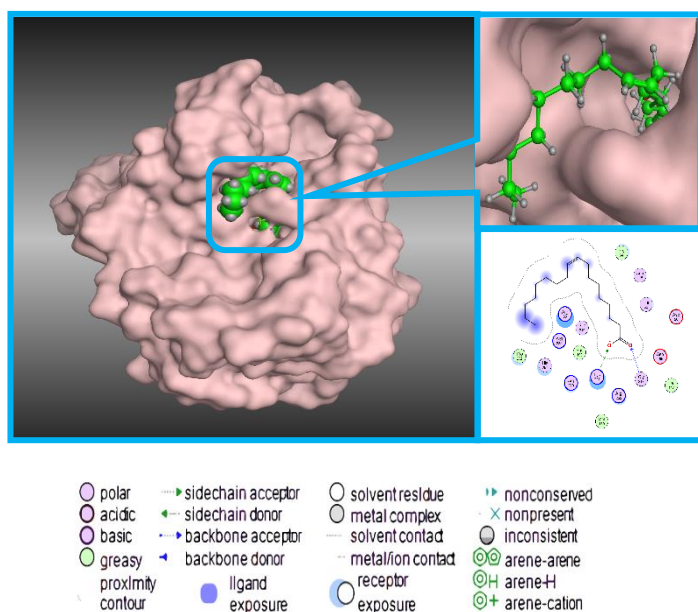


**Figure 4:** (a) Surface and (b) 2D view of docked conformation of *Ij* against *E. coli* 1AJ0 protein

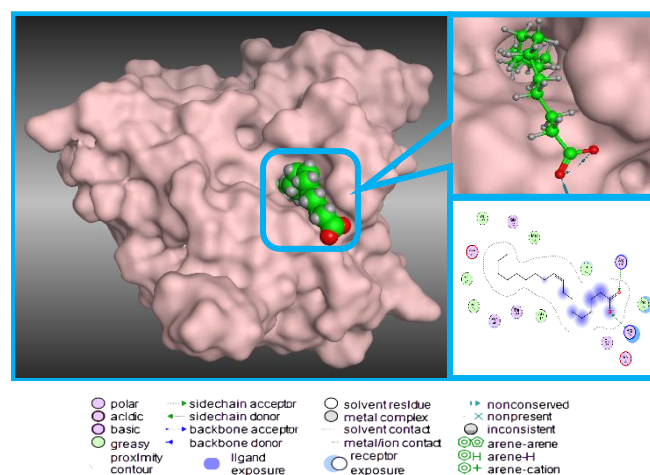


**Figure 5:** (a) Surface and (b) 2D view of docked conformation of *Ig* against *E. coli* 6F86 protein

Table 2 displays the various binding energies that were obtained when the *S. aureus* proteins TyrRS and DNA gyrase B were docked with the binding sites of the same ligands. For the TyrRS protein and the DNA gyrase B protein, the sixteen phytochemical compounds' S-scores ranged from -5.06 to -9.07 and -4.41 to -7.30 kcal/mol, respectively. In contrast, the conventional ceftriaxone produced S-score values of -9.53 and -7.54 kcal/mol with the same two proteins, respectively. The highest docked ligands with DNA gyrase B protein were *Ij* (-7.30 kcal/mol) and *Il* (-7.27 kcal/mol). Of the docked ligands, *Ig*, *Ii*, *Ij*, *Il*, and *Im* had a high S-score (-7.21, -7.41, -9.07, -7.94, and -7.82 kcal/mol, respectively) against the TyrRS protein. With TyrRS protein, ligand *Ig* connected with the protein post by ionic and hydrogen interactions with LYS84 and ARG88 (Table 4 and Figure 7), whereas ligand *Il* interacted through ionic and hydrogen bonds with ASP80, ARG88, and LYS84 (Table 4 and Figure 8). As seen in Table 4 and Figure 9, ligand *Ig* also had an H-bond with LYS84 and ionic interactions with LYS84 and ARG88 for the DNA gyrase B, whereas ligand *Il* provided two H-connections with ARG144 and two ionic bonds with the same amino acids for the same protein (Table 4 and Figure 10).

In the Drug-Likeness and ADMET properties studies, tools from ADMETlab were utilized to examine the physicochemical and drug-like properties. When the chemical meets the appropriate criteria—

molecular weight  $\leq 500$  g/mol,  $\log P \leq 5$ , number of hydrogen bond acceptors  $\leq 10$ , and number of hydrogen bond donors  $\leq 5$  it can be a superior clinical candidate, according to Lipinski's Rules of Five.<sup>36-38</sup> According to Table 5, the chosen compounds' molecular weights fall within the permissible range of  $\leq 500$  g/mol, this is significant because high molecular weights can affect the body's ability to absorb, diffuse,

and transport substances.<sup>39</sup> Selected chemicals have superior solubility in cellular membranes because their number of hydrogen bond donors is fewer than 5 and their number of hydrogen bond acceptors is less than 10. According to the outcome, every chosen compound complies with Lipinski's Five Rules.

**Table 4:** Molecular docking data of phytochemicals against *S. aureus* proteins

Compd	1JJJ protein				3G75 protein				
	Ligand- Amino acid Interaction	Types of Interactions	Distance (Å)	Interaction Energy (kcal/mol)	Ligand-Amino acid Interaction	Types of Interactions	Distance (Å)	Interaction Energy (kcal/mol)	
<i>Ia</i>	O6 – TYR36	H-acceptor	3.44	-28.74	O6 – SER 129	H-acceptor	2.76	-26.70	
<i>Ib</i>	O31 – GLN190	H-acceptor	2.75	-13.82	O31 – THR173	H-acceptor	2.95	-25.14	
<i>Ic</i>	O30 – ASP40	H-donor	2.73	-28.03	O34 – THR173	H-acceptor	2.77	-22.61	
	O34 – GLN190	H-acceptor	2.76						
<i>Id</i>	O21 – CYS37	H-donor	4.10	-23.84	O21 – THR173	H-acceptor	2.85	-24.05	
	O21 – GLY193	H-acceptor	3.42						
<i>Ie</i>	O12 – LYS84	H-acceptor	2.81	-24.23	O17 – HIS50	H-pi	3.89	-19.01	
	O17 – HIS50	H-pi	3.89						
<i>If</i>	O15 – TYR36	H-acceptor	2.97	-32.33	O14 – THR173	H-acceptor	2.89	-21.79	
<i>Ig</i>	O49 – LYS84	H-acceptor	3.10	-35.33	O48 – ARG84	H-acceptor	3.49	-36.82	
	O49 – LYS84	Ionic	3.10		O49 – ARG144	H-acceptor	2.98		
	O49 – ARG88	Ionic	3.89		O49 – ARG144	Ionic	2.98		
<i>Ih</i>	O37 – LYS84	H-acceptor	2.97	-27.20				-22.20	
<i>Ii</i>	C67 – HIS50	H-pi	3.99	-30.01				-27.54	
<i>Ij</i>				-42.67				-39.15	
<i>Ik</i>	CL11 – ASP80	H-donor	3.22	-23.08	CL11 – ASP57	H-donor	3.94	-22.44	
	O10 – ASP40	H-acceptor	2.84						
<i>Il</i>	O52 – ASP80	H-acceptor	3.57	-38.66	O52 – ARG144	H-acceptor	2.96	-36.69	
	O52 – ARG88	H-acceptor	2.89		O53 – ARG144	H-acceptor	2.99		
	O53 – LYS84	H-acceptor	2.86		O52 – ARG144	Ionic	2.96		
	O52 – ARG88	Ionic	2.89		O53 – ARG144	Ionic	2.99		
	O53 – LYS84	Ionic	2.86						
	O53 – ARG88	Ionic	3.13						
<i>Im</i>	C51 – HIS50	H-pi	3.45	-31.62				-27.96	
<i>In</i>	C23 – ASP177	H-donor	3.11	-33.25	O19 – ARG144	H-acceptor	3.28	-29.96	
	O20 – GLY193	H-acceptor	2.93						
<i>Io</i>	C14 – ASP195	H-donor	3.39	-22.38				-17.08	
	C9 – PHE54	H-pi	4.79						
<i>Ip</i>	6-ring – ALA39	pi-H	4.27	-32.27				-22.08	

**Table 5:** *In silico* physicochemical and drug-likeness properties of isolated compounds

Parameter	<i>Ia</i>	<i>Ib</i>	<i>Ic</i>	<i>Id</i>	<i>Ie</i>	<i>If</i>	<i>Ig</i>	<i>Ih</i>
Molecular Weight (MW)	288.140	230.130	248.140	230.130	218.130	231.050	256.240	248.140
Van der Waals volume (VDWV)	249.361	249.361	260.788	249.361	234.702	226.698	300.236	260.788
Density (MW/VDWV)	0.964	0.923	0.952	0.923	0.929	1.019	0.853	0.952
H-bond Acceptor Count	4	2	3	2	2	5	2	3
H-bond Donor Count	0	0	1	0	0	0	1	1
Rotatable Bond Count	2	0	0	0	0	1	14	0
Molecular Flexibility	0.100	0.000	0.000	0.000	0.000	0.071	14.000	0.000
Stereo Centers Count	5	4	5	4	0	0	0	5
TPSA	52.600	26.300	46.530	26.300	34.140	77.280	37.300	46.530
Water solubility Log S	-2.877	-3.612	-3.216	-3.458	-1.802	-4.196	-5.223	-3.087
Lipophilicity Log P <sub>ow</sub>	1.722	2.759	2.160	3.516	1.312	2.356	6.732	2.660

References, MW < 500, H-bond Acceptor Count = < 10, H-bond Donor Count < 5, Rotatable Bond Count < 11, Stereo Centers Count  $\leq 2$ , TPSA  $\leq 140$ , Log S -4 to 0.5, log P < 5

**Table 5 Cont'd:** *In silico* physicochemical and drug-likeness properties of isolated compounds

Parameter	<i>Ii</i>	<i>Ij</i>	<i>Ik</i>	<i>Il</i>	<i>Im</i>	<i>In</i>	<i>Io</i>	<i>Ip</i>
Molecular Weight (MW)	414.390	430.380	266.140	282.260	278.300	246.130	246.130	244.180
Van der Waals volume (VDWV)	482.068	502.698	290.191	332.192	349.203	258.152	258.152	283.720
Density (MW/VDWV)	0.860	0.856	0.917	0.850	0.797	0.953	0.953	0.861

H-bond Acceptor Count	1	2	1	2	0	3	3	1
H-bond Donor Count	1	1	0	1	0	0	0	0
Rotatable Bond Count	6	12	4	15	13	0	0	2
Molecular Flexibility	0.300	1.091	0.571	7.500	6.500	0.000	0.000	0.182
Stereo Centers Count	9	3	0	0	2	4	4	0
TPSA	20.230	29.460	17.070	37.300	0.000	35.530	35.530	17.070
Water solubility Log S	-7.052	-6.995	-5.843	-3.308	-7.116	-2.777	-2.777	-5.593
Lipophilicity Log P <sub>o/w</sub>	7.663	9.852	4.959	6.169	8.007	2.282	2.282	5.556

Standard, MW < 350, H-bond Acceptor Count = < 12, H-bond Donor Count < 7, Rotatable Bond Count < 11, Stereo Centers Count ≤ 2, TPSA ≤ 140, Log S -4 to 0.5, log P < 5

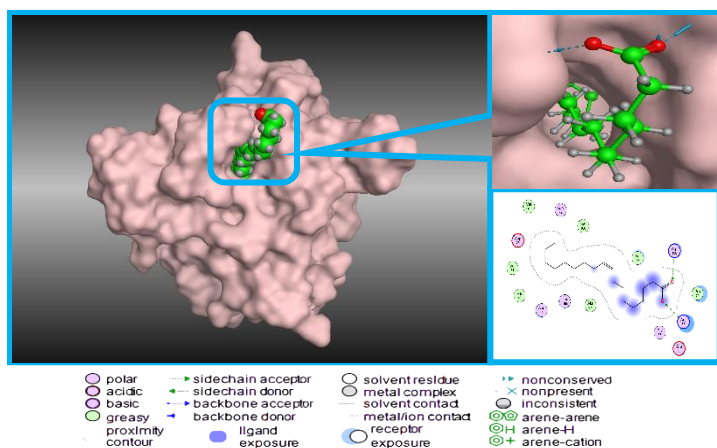


**Figure 6:** (a) Surface and (b) 2D view of docked conformation of *11* against *E. coli* 6F86 protein

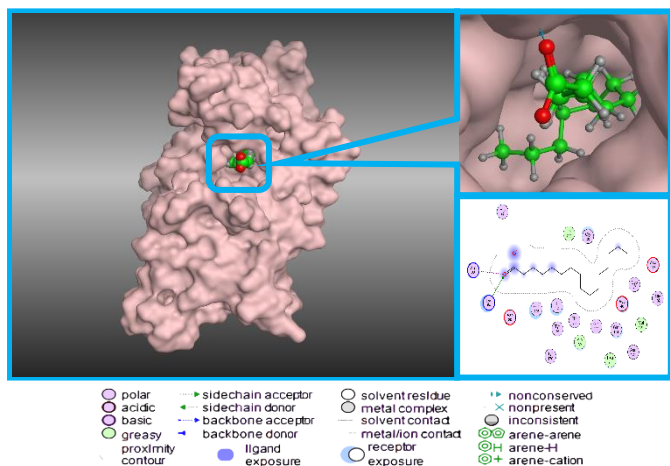


**Figure 7:** (a) Surface and (b) 2D view of docked conformation of *1g* against *S. aureus* 1JJJ protein

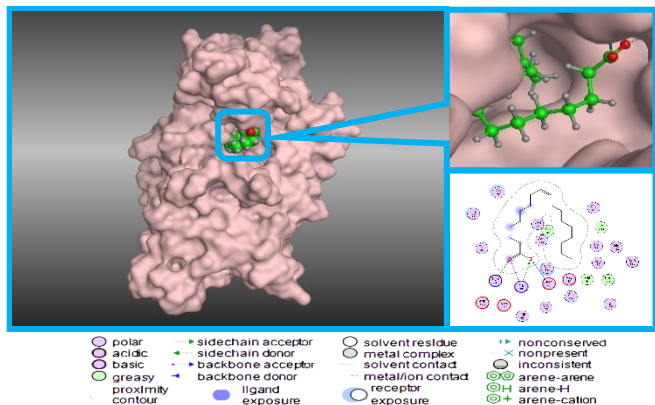


**Figure 10:** (a) Surface and (b) 2D view of docked conformation of *11* against *S. aureus* 3G75 protein.

**Figure 8:** (a) Surface and (b) 2D view of docked conformation of *11* against *S. aureus* 1JJJ protein

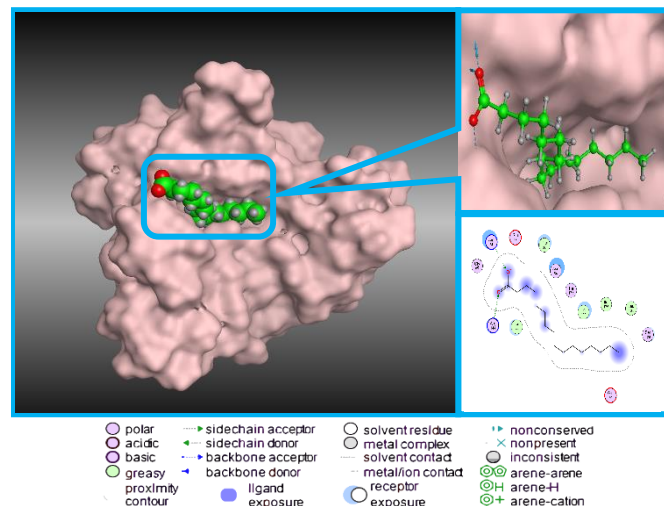


**Figure 9:** (a) Surface and (b) 2D view of docked conformation of *1g* against *S. aureus* 3G75 protein

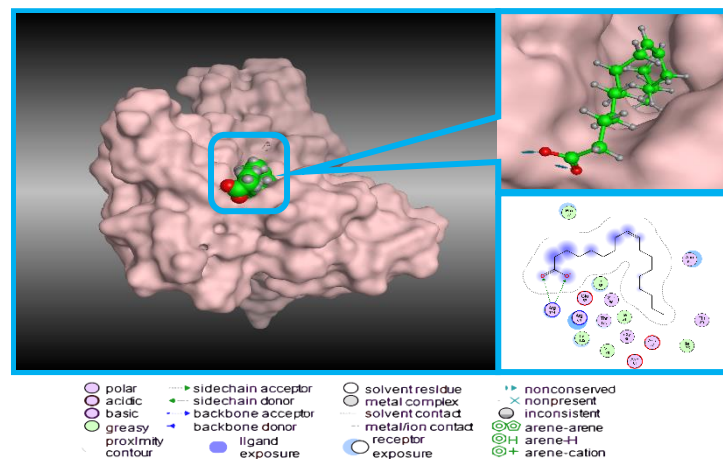


**Figure 10:** (a) Surface and (b) 2D view of docked conformation of *11* against *S. aureus* 3G75 protein.

Lipophilicity (logP) values less than five, a favourable indicator of oral availability<sup>40</sup>, were present in 60% of the compounds that were chosen. The consensus log P<sub>o/w</sub> was taken into consideration when calculating the mean anticipated lipophilicity values, which were used to determine the compound's non-aqueous solubility. This means that the consensus log P<sub>o/w</sub> values of a molecule will be more negative the more soluble it is. Findings indicated that the substance is not soluble in non-aqueous media, and the log S scale was employed to calculate the aqueous solubility, the chemical is moderately soluble (-7.116 to -1.802) on the log S scale. If log S is less than or equal to ten in the following cases:

poorly soluble, moderately soluble, soluble, extremely soluble, and highly soluble at or below 0.6.<sup>41</sup>

The compounds' topological polar surface area (TPSA) ranged from 17.070 to 77.280 Å<sup>2</sup>, which is less than 140 Å<sup>2</sup>, indicating acceptable solubility.<sup>42</sup> Better permeability through the gastrointestinal and blood-brain barriers is suggested by lower TPSA readings. A novel drug candidate may be identified by having rotatable bonds less than nine<sup>43</sup>; nevertheless, this criterion does not satisfy nearly all phytochemicals, except for *1a*, *1f*, *1i*, *1k*, and *1p*. Molecular flexibility is reflected in the values of rotatable bonds and ranges from 0.0 (stiff) to 1.0 (fully flexible).<sup>44</sup>

Table 6 presents the estimated pharmacokinetic parameters of the separated compounds in terms of ADME (Absorption, Distribution, Metabolism, and Excretion), which offers information on their possible therapeutic use. For all phytochemical substances, gastrointestinal (GI) absorption exhibited improved absorption kinetics. All compounds showed strong Caco-2 membrane permeability (log Papp value > 0.9 cm/s)<sup>45</sup>, suggesting that they might be absorbed by humans. Except for *1a*, *1f*, *1g*, *1l*, and *1p*, the skin permeability values for certain substances were below the typical threshold (log kp ≥ -2.5 cm/s)<sup>46</sup>, indicating poor absorptive capacities through the skin. *1e* and *1n* were shown to be substrates for P-gp, which may affect how well they are absorbed and distributed throughout the body with their interaction with P-glycoprotein (P-gp). On the other hand, *1i* and *1j* were found to be P-gp II inhibitors, which may have an impact on their systemic distribution and bioavailability. In contrast, *1a*, *1b*, and *1d* were shown to be P-gp I.<sup>47,48</sup> The ability of the compounds to diffuse and penetrate via different physiological barriers was studied (Table 6). Except for *1g* and *1l*, all substances had steady-state volume of distribution (VDss) values that were greater than the lower limit (> -0.15), demonstrating their wide dispersion throughout the body. In contrast to the other compounds, *1j*, *1k*, *1m*, and *1p* showed greater VDss values (>0.45), indicating that they were distributed widely throughout tissues as opposed to in the plasma.<sup>49</sup> For 70% of the compounds, a greater unbound fraction was found, suggesting improved cell membrane penetration. On the other hand, 30% of compounds showed a zero unattached fraction, indicating

a high affinity for protein binding. The ability of phytochemicals (56%) to cross the blood-brain barrier (BBB) is demonstrated by log BB values > 0.3<sup>50</sup>, and 87% of these compounds are distributed in the central nervous system (CNS) as indicated by log PS values > -2<sup>51</sup>, suggesting that these compounds may have neurological effects.

By evaluating the separated compounds' interactions with cytochrome P450 isoforms and taking into account their functions as substrates or inhibitors, metabolism prediction was carried out (Table 5). For all isoenzymes, the majority of the substances were found to be noninhibited. Nevertheless, it was shown that 68% of the substances are substrates for CYP3A4 isoenzymes, suggesting that CYP3A4 may be involved in the modification of some metabolic pathways. None of the substances were anticipated to be substrates for the renal organic cation transporter 2 (OCT2) in terms of excretion kinetics. While *1k* had the lowest score (-0.08 logmL/min/kg)<sup>52</sup>, indicating a relatively low clearance rate, 93% of chemicals showed the maximum overall clearance score (0.3-1.884 log mL/min/kg), demonstrating their effective removal from the body. The majority of chemicals' safety profiles are shown by the toxicity evaluations listed in Table 7. Class 6 (LD<sub>50</sub> > 5000) was assigned to compound *1m*, suggesting that it is comparatively non-toxic. Comparably, class 5 (2000 < LD<sub>50</sub> ≤ 5000) was assigned to *1e*, *1f*, *1h*, and *1j*, emphasizing their low toxicity. However, class 4 (300 < LD<sub>50</sub> ≤ 2000) include *1a*, *1b*, *1c*, *1d*, *1g*, *1i*, *1k*, *1n*, *1o*, and *1p*, which show a higher level of toxicity. All of the isolated compounds are very similar in acute rat oral toxicity (LD<sub>50</sub>) estimates, which range from 1.533 to 2.674 mol/kg.<sup>53,54</sup>

Compound *1a* showed greater hazardous values (0.829 log mg/kg/day) in chronic rat oral toxicity than the other compounds, indicating possible long-term health hazards associated with their use. Only three of the sixteen compounds identified in the identification state function as hERGII inhibitors, which raises questions regarding their possible effects on cardiac health. Finally, the lack of identification as hERGI inhibitors is a favorable discovery. The hepatotoxicity results showed that all of the compounds, except *1l* and *1n*, are benign. The skin sensitization results indicated that half of the compounds are safe.<sup>55,56</sup>

**Table 6:** ADME pharmacokinetic properties of the phytochemical compounds

Parameters	Phytochemicals							
	<i>1a</i>	<i>1b</i>	<i>1c</i>	<i>1d</i>	<i>1e</i>	<i>1f</i>	<i>1g</i>	<i>1h</i>
Absorption								
Caco2 permeability	1.373	1.089	1.269	1.919	1.602	0.959	1.557	1.283
GI absorption	98.735	99.15	97.186	98.315	97.85	96.679	91.957	97.522
Skin Permeability	-3.26	-2.579	-3.678	-2.436	-2.864	-2.476	-2.371	-2.94
P-gp substrate (Yes/No)	No	No	No	No	Yes	No	No	No
P-gp I inhibitor (Yes/No)	Yes	Yes	No	Yes	No	No	No	No
P-gp II inhibitor (Yes/No)	No	No	No	No	No	No	No	No
Distribution								
VDss (human)	0.09	0.323	0.222	0.355	0.333	0.232	-0.56	0.193
Fraction unbound (human)	0.337	0.277	0.456	0.251	0.482	0.208	0.094	0.391
BBB permeant	-0.235	0.6	0.343	0.591	0.311	-0.251	-0.119	-0.002
CNS permeability	-2.817	-2.207	-2.903	-2.167	-3.093	-2.121	-1.816	-2.617
Metabolism								
CYP2D6 substrate	No	No	No	No	No	No	Yes	No
CYP3A4 substrate	Yes	Yes	No	Yes	No	No	Yes	No
CYP1A2 inhibitor	No	No	Yes	No	No	Yes	Yes	No
CYP2C19 inhibitor	No	No	No	No	No	No	No	No
CYP2C9 inhibitor	No	No	No	No	No	No	No	No
CYP2D6 inhibitor	No	No	No	No	No	No	No	No
CYP3A4 inhibitor	No	Yes	No	No	No	No	No	No
Excretion								
Total renal clearance	0.685	0.691	1.158	0.693	1.197	0.405	1.763	1.142
Renal OCT2 substrate	Yes	Yes	No	Yes	No	No	No	No

OCT2 = Organic Cation Transporter 2, BBB = Blood-brain barrier, CNS = Central nervous system, P-gp = P-glycoprotein, VDss = steady-state volume of distribution

**Table 6 Cont'd:** ADME pharmacokinetic properties of the phytochemical compounds

	Phytochemicals							
	<i>Ii</i>	<i>Ij</i>	<i>Ik</i>	<i>Il</i>	<i>Im</i>	<i>In</i>	<i>Io</i>	<i>Ip</i>
Absorption								
Caco2 permeability	1.205	1.219	1.306	1.562	1.397	1.306	1.701	1.524
GI absorption	94.866	89.181	94.102	91.776	91.794	95.005	98.926	95.313
Skin Permeability	-2.794	-2.699	-2.562	-2.522	-2.575	-3.123	-2.932	-2.011
P-gp substrate (Yes/No)	No	No	No	No	No	Yes	No	No
P-gp I inhibitor (Yes/No)	No	No	No	No	No	No	No	No
P-gp II inhibitor (Yes/No)	Yes	Yes	No	No	Yes	No	No	No
Distribution								
VDss (human)	0.24	0.744	0.888	-0.567	0.639	0.311	0.307	0.841
Fraction unbound (human)	0	0	0	0.046	0	0.139	0.366	0
BBB permeant	0.797	0.962	0.719	-0.176	0.96	0.269	0.146	0.574
CNS permeability	-1.754	-1.629	-1.28	-1.654	-1.296	-1.727	-2.716	-1.408
Metabolism								
CYP2D6 substrate	No	No	No	Yes	No	No	No	No
CYP3A4 substrate	Yes	Yes	Yes	Yes	Yes	Yes	No	Yes
CYP1A2 inhibitor	No	No	Yes	Yes	Yes	Yes	Yes	Yes
CYP2C19 inhibitor	No	No	No	No	No	Yes	No	Yes
CYP2C9 inhibitor	No	No	No	No	No	No	No	No
CYP2D6 inhibitor	No	No	No	No	No	No	No	No
CYP3A4 inhibitor	No	No	No	No	No	No	No	No
Excretion								
Total renal clearance	0.628	0.798	-0.008	1.884	1.764	0.3	0.605	0.954
Renal OCT2 substrate	No	No	No	No	No	No	No	No

**Table 7:** Toxicity properties of the phytochemical compounds

Parameters	Phytochemicals							
	<i>Ia</i>	<i>Ib</i>	<i>Ic</i>	<i>Id</i>	<i>Ie</i>	<i>If</i>	<i>Ig</i>	<i>Ih</i>
AMES toxicity	No	No	No	No	No	Yes	No	No
Max. tolerated dose (human) (log mg/kg/day)	0.035	0.349	0.423	0.112	0.318	0.192	-0.818	0.228
hERG I inhibitor	No	No	No	No	No	No	No	No
hERG II inhibitor	No	No	No	No	No	No	No	No
Oral Rat Acute Toxicity (LD <sub>50</sub> ) (mol/kg)	1.997	1.638	1.838	1.72	1.85	2.053	1.595	2.278
Oral Rat Chronic Toxicity (LOAEL) (log mg/kg bw/ day)	1.371	1.805	1.605	1.794	1.797	1.598	3.173	1.727
Hepatotoxicity	No	No	No	No	No	No	No	No
Skin Sensitization	No	Yes	No	Yes	Yes	No	Yes	No
<i>T. Pyriformis</i> toxicity (log µg/L)	0.692	0.92	0.698	1.17	0.466	1.47	0.387	0.613
Minnow toxicity (log mM)	1.947	1.244	1.989	1.148	1.597	0.538	-1.083	1.44
Predicted LD50 (mg/kg)	1330	1330	1330	1330	5000	3000	900	5000
Predicted Toxicity Class	4	4	4	4	5	5	4	5

hERG = human ether-go-go-related gene

**Table 7 Cont'd** Toxicity properties of the phytochemical compounds

Parameters	Phytochemicals							
	<i>Ii</i>	<i>Ij</i>	<i>Ik</i>	<i>Il</i>	<i>Im</i>	<i>In</i>	<i>Io</i>	<i>Ip</i>
AMES toxicity	No	No	No	No	No	No	No	No
Max. tolerated dose (human) (log mg/kg/day)	-0.555	0.595	-0.126	-0.943	-0.066	-0.265	0.369	0.106
hERG I inhibitor	No	No	No	No	No	No	No	No
hERG II inhibitor	Yes	Yes	No	No	Yes	No	No	No
Oral Rat Acute Toxicity (LD <sub>50</sub> ) (mol/kg)	2.326	1.965	1.748	1.604	1.533	2.658	2.674	1.905
Oral Rat Chronic Toxicity (LOAEL) (log mg/kg bw/ day)	0.829	2.365	1.248	3.251	1.137	1.891	1.751	1.18
Hepatotoxicity	No	No	No	Yes	No	Yes	No	No

Skin Sensitization	No	No	Yes	Yes	Yes	No	No	Yes
<i>T. Pyriformis</i> toxicity (log µg/L)	0.454	0.979	0.506	0.366	1.5	1.521	0.673	2.334
Minnnow toxicity (log mM)	-2.12	-3.281	-1.222	-1.438	-1.871	0.916	1.193	-0.183
Predicted LD50 (mg/kg)	890	5000	2000	48	5050	330	1330	1700
Predicted Toxicity Class	4	5	4	2	6	4	4	4

## Conclusion

*Lawsonia inermis* acetone extract exhibited inhibitory potential against bacteria isolated from urinary tract infections (UTIs) and wound infections, including *E. Coli*, *K. pneumonia*, *P. aeruginosa*, and *S. aureus*. *Lawsonia inermis* extract contains sixteen different phytochemicals, some of which have demonstrated their antibacterial action and obeyed ADMET and Lipinski rules. The most promising possibilities among these sixteen compounds, based on *in silico* investigations, were *Ig* (n-Hexadecanoic acid) and *Il* (Oleic Acid), which demonstrated significant affinity (S-score) with the four categories of bacterial proteins. Additionally, some of these substances showed superior molecular interactions to the generic ceftriaxone medication. Consequently, the study concluded that antibiotic resistance was on the rise, but that plant extract phytochemicals had a wider range of antibacterial activity, which may open the door to the development of alternative medicines derived from natural sources.

## Conflict of Interest

The authors declare no conflict of interest.

## Authors' Declaration

The authors hereby declare that the work presented in this article is original and that any liability for claims relating to the content of this article will be borne by them.

## References

- Rabizadeh F, Mirian MS, Doosti R, Kiani-Anbouhi R, Eftekhari E. Phytochemical classification of medicinal plants used in the treatment of kidney disease based on traditional Persian medicine. *Evid. Comp. Alter. Med.* 2022; 2022(1):8022599. <https://doi.org/10.1155/2022/8022599>
- Kumar A, P N, Kumar M, Jose A, Tomer V, Oz E, Proestos C, Zeng M, Elobeid T, K S, Oz F. Major phytochemicals: recent advances in health benefits and extraction method. *Molecules.* 2023; 28(2):887. <https://doi.org/10.3390/molecules28020887>
- Iriti M, Faoro F. Chemical diversity and defence metabolism: how plants cope with pathogens and ozone pollution. *Inter. J. Mol. Sci.* 2009; 10(8):3371-3399. <https://doi.org/10.3390/ijms10083371>
- Rodríguez-Negrete EV, Morales-González Á, Madrigal-Santillán EO, Sánchez-Reyes K, Álvarez-González I, Madrigal-Bujaidar E, Valadez-Vega C, Chamorro-Cevallos G, Garcia-Melo LF, Morales-González JA. Phytochemicals and Their Usefulness in the Maintenance of Health. *Plants.* 2024; 13(4):523. <https://doi.org/10.3390/plants13040523>
- Goswami C, Pawase PA, Shams R, Pandey VK, Tripathi A, Rustagi S, Darshan G. A Conceptual Review on Classification, Extraction, Bioactive Potential and Role of Phytochemicals in Human Health. *Future Foods.* 2024; 9:100313. <https://doi.org/10.1016/j.fufo.2024.100313>
- Ekor M. The growing use of herbal medicines: issues relating to adverse reactions and challenges in monitoring safety. *Front Pharm.* 2014; 4:177. <https://doi.org/10.3389/fphar.2013.00177>
- Franco GA, Interdonato L, Cordaro M, Cuzzocrea S, Di Paola R. Bioactive compounds of the Mediterranean diet as nutritional support to fight neurodegenerative disease. *Inter. J. Mol. Sci.* 2023; 24(8):7318. <https://doi.org/10.3390/ijms24087318>
- He WJ, Lv CH, Chen Z, Shi M, Zeng CX, Hou DX, Qin S. The regulatory effect of phytochemicals on chronic diseases by targeting Nrf2-ARE signaling pathway. *Antioxidants.* 2023; 12(2):236. <https://doi.org/10.3390/antiox12020236>
- Ceramella J, De Maio AC, Basile G, Facente A, Scali E, Andreu I, Sinicropi MS, Iacopetta D, Catalano A. Phytochemicals involved in mitigating silent toxicity induced by heavy metals. *Foods.* 2024; 13(7):978. <https://doi.org/10.3390/foods13070978>
- Siddiqui SA, Azmy Harahap I, Suthar P, Wu YS, Ghosh N, Castro-Muñoz R. A comprehensive review of phytonutrients as a dietary therapy for obesity. *Foods.* 2023; 12(19):3610. <https://doi.org/10.3390/foods12193610>
- Habbal O, Hasson SS, El-Hag AH, Al-Mahrooqi Z, Al-Hashmi N, Al-Bimani Z, Al-Balushi MS, Al-Jabri AA. Antibacterial activity of *Lawsonia inermis* Linn (Henna) against *Pseudomonas aeruginosa*. *Asia. Paci. J. Trop. Biomed.* 2011; 1(3):173-176. [https://doi.org/10.1016/S2221-1691\(11\)60021-X](https://doi.org/10.1016/S2221-1691(11)60021-X)
- Moutawalli A, Benkhoulil FZ, Doukkali A, Benzeid H, Zahidi A. The biological and pharmacologic actions of *Lawsonia inermis* L. *Phytomed. Plus.* 2023; 3(3):100468. <https://doi.org/10.1016/j.phyplu.2023.100468>
- Batiha GE, Teibo JO, Shaheen HM, Babalola BA, Teibo TK, Al-Kuraishy HM, Al-Garbeeb AI, Alexiou A, Papadakis M. Therapeutic potential of *Lawsonia inermis* Linn: a comprehensive overview. *Naunyn-schmiedeberg's Arch. Pharm.* 2024; 397(6):3525-3540. <https://doi.org/10.1007/s00210-023-02735-8>
- Kumar M, Kaur P, Chandel M, Singh AP, Jain A, Kaur S. Antioxidant and hepatoprotective potential of *Lawsonia inermis* L. leaves against 2-acetylaminofluorene induced hepatic damage in male Wistar rats. *BMC Comp. Alter. Med.* 2017; 17:1-11. <https://doi.org/10.1186/s12906-017-1567-9>
- Zibanejad S, Miraj S, Kopaei MR. Healing effect of *Quercus persica* and *Lawsonia inermis* ointment on episiotomy wounds in primiparous women. *J. Res. Med. Sci.* 2020; 25(1):11. [https://doi.org/10.4103/jrms.JRMS\\_251\\_18](https://doi.org/10.4103/jrms.JRMS_251_18)
- Talab TA, Alfuraiji N, Al-Snafi AE. The analgesic and anti-inflammatory effect of Lawsone isolated from *Lawsonia inermis*. *ScienceRise: Pharm. Sci.* 2022; 1(35):77-84. <https://doi.org/10.15587/2519-4852.2022.253555>
- Balaei-Kahnamoei M, Saedi M, Rastegari A, Shams Ardekani MR, Akbarzadeh T, Khanavi M. Phytochemical analysis and evaluation of biological activity of *Lawsonia inermis* Seeds related to Alzheimer's disease. *Evid. Comp. Alter. Med.* 2021; 2021(1):5965061. <https://doi.org/10.1155/2021/5965061>
- Batiha GE, Teibo JO, Shaheen HM, Babalola BA, Teibo TK, Al-Kuraishy HM, Al-Garbeeb AI, Alexiou A, Papadakis M. Therapeutic potential of *Lawsonia inermis* Linn: a comprehensive overview. *Naunyn-schmiedeberg's Arch. Pharm.* 2024; 397(6):3525-3540. <https://doi.org/10.1007/s00210-023-02735-8>
- Al-Rubiy KK, Jaber NN, Al-Mhaawe BH, Alrubaiy LK. Antimicrobial efficacy of henna extracts. *Oman Med. J.* 2008; 23(4):253-256. <https://pubmed.ncbi.nlm.nih.gov/articles/PMC3273913/>
- Jasim EQ, Muhammad-Ali MA, Almakki A. Synthesis, characterization, and antibacterial activity of some mesalazine derivatives. *Sci. Tech. Ind.* 2023; 8(3):338-343. <https://doi.org/10.26554/sti.2023.8.3.338-343>
- Hayat J, Akodad M, Moumen A, Baghour M, Skalli A, Ezrari S, Belmalha S. Phytochemical screening, polyphenols, flavonoids and tannin content, antioxidant activities and FTIR characterization of *Marrubium vulgare* L. from 2 different localities of Northeast of Morocco. *Heliyon.* 2020; 6(11). <https://doi.org/10.1016/j.heliyon.2020.e05609>
- Kancherla N, Dhakshinamoorthy A, Chitra K, Komaram RB. Preliminary analysis of phytoconstituents and evaluation of anthelmintic property of *Cayratia auriculata* (in vitro). *Maedica.* 2019; 14(4):350. <https://pubmed.ncbi.nlm.nih.gov/articles/PMC7035446/>
- Utami YP, Yulianty R, Djabir YY, Alam G. Antioxidant Activity, Total Phenolic and Total Flavonoid Contents of *Etlingera elatior* (Jack) RM Smith from North Luwu, Indonesia. *Trop. J. Nat. Prod. Res.* 2024; 8(1):5955-5961. <http://www.doi.org/10.26538/tjnp/v8i1.34>

24. Okafor CE, Ijoma IK, Igboamalu CA, Ezebalu CE, Eze CF, Osita-Chikeze JC, Uzor CE, Ekwuekwe AL. Secondary metabolites, spectra characterization, and antioxidant correlation analysis of the polar and nonpolar extracts of *Bryophyllum pinnatum* (Lam) Oken. *BioTechnologia*. 2024; 105(2):121-136. <https://doi.org/10.5114/bta.2024.139752>
25. Jasim EQ, Muhammad-Ali MA, Al-Abdullah AA. In Vitro Studies of Biosynthesized Nanoparticles of *Dysphania* Aqueous Leaves Extract Against Some Isolated Bacteria from Wounds and Burns and *In Silico* Evaluations of Compounds Identified in its GC-MS Spectra. *Trop. J. Nat. Prod. Res.* 2024; 8(11):9155 – 9165. <https://doi.org/10.26538/tjnpr/v8i11.26>
26. Mendie LE, Hemalatha S. Molecular docking of phytochemicals targeting GFRs as therapeutic sites for cancer: an *in silico* study. *Appl. Biochem. Biotechnol.* 2022; 194(1):215-231. <https://doi.org/10.1007/s12010-021-03791-7>
27. Asha RN, Nayagam BR, Bhuvanesh N. Synthesis, molecular docking, and *in silico* ADMET studies of 4-benzyl-1-(2, 4, 6-trimethyl-benzyl)-piperidine: Potential Inhibitor of SARS-CoV2. *Bioorg. Chem.* 2021; 112:104967. <https://doi.org/10.1016/j.bioorg.2021.104967>
28. Uzzaman M, Hasan MK, Mahmud S, Fatema K, Matin MM. Structure-based design of new diclofenac: Physicochemical, spectral, molecular docking, dynamics simulation, and ADMET studies. *Inform. Med. Unlocked.* 2021; 25:100677. <https://doi.org/10.1016/j.imu.2021.100677>
29. Sartori SK, Diaz MA, Diaz-Muñoz G. Lactones: Classification, synthesis, biological activities, and industrial applications. *Tetrahedron.* 2021; 84:132001. <https://doi.org/10.1016/j.tet.2021.132001>
30. Edan DJ, Muhammad-Ali MA, Jaafar RS. Combined Efficacy of *Lawsonia inermis* and *Myrtus communis* Extract as a Potential Factor in Bacterial Treatment to Hospital Wastewater, Iraq. *INOP Conf. Ser.: Ear. Envi. Sci.* 2023; 1215(1):012008. <https://doi.org/10.1088/1755-1315/1215/1/012008>
31. Güler Ş, Torul D, Kurt-Bayraktar S, Tayyarcan EK, Çamsarı Ç, Boyacı İH. Evaluation of antibacterial efficacy of *Lawsonia inermis* Linn (henna) on periodontal pathogens using agar well diffusion and broth microdilution methods: an *in-vitro* study. *BioMedicine*. 2023; 13(3):25. <https://doi.org/10.37796/2211-8039.1411>
32. Vanlalveni C, Lallianrawna S, Biswas A, Selvaraj M, Changmai B, Rokhum SL. Green synthesis of silver nanoparticles using plant extracts and their antimicrobial activities: A review of recent literature. *RSC advances.* 2021; 11(5):2804-2837. <https://doi.org/10.1039/D0RA09941D>
33. Mazur M, Masłowiec D. Antimicrobial activity of lactones. *Antibiotics.* 2022; 11(10):1327. <https://doi.org/10.3390/antibiotics11101327>
34. Mundt S, Kreitlow S, Jansen R. Fatty acids with antibacterial activity from the cyanobacterium *Oscillatoria redekei* HUB 051. *J. Appl. Phys.* 2003; 15:263-267. <https://doi.org/10.1023/A:1023889813697>
35. Dahlem Junior MA, Nguema Edzang RW, Catto AL, Raimundo JM. Quinones as an efficient molecular scaffold in the antibacterial/antifungal or antitumoral arsenal. *Inter. J. Mol. Sci.* 2022; 23(22):14108. <https://doi.org/10.3390/ijms232214108>
36. Gheidari D, Mehrdad M, Bayat M. Synthesis, docking, MD simulation, ADMET, drug-likeness, and DFT studies of novel furo [2, 3-b] indol-3a-ol as promising Cyclin-dependent kinase 2 inhibitors. *Sci. Rep.* 2024; 14(1):3084. <https://doi.org/10.1038/s41598-024-53514-1>
37. Ibrahim ZY, Uzairu A, Shallangwa G, Abechi S. Molecular docking studies, drug-likeness, and *in-silico* ADMET prediction of some novel  $\beta$ -Amino alcohol grafted 1,4,5-trisubstituted 1,2,3-triazoles derivatives as elevators of p53 protein levels. *Sci. Afr.* 2020; 10:e00570. <https://doi.org/10.1016/j.sciaf.2020.e00570>
38. Ononamadu CJ, Ibrahim A. Molecular docking and prediction of ADME/drug-likeness properties of potentially active antidiabetic compounds isolated from aqueous-methanol extracts of *Gymnema sylvestris* and *Combretum micranthum*. *BioTechnologia*. 2021; 102(1):85. <https://doi.org/10.5114/bta.2021.103765>
39. Yang NJ, Hinner MJ. Getting across the cell membrane: an overview for small molecules, peptides, and proteins. *Site-Specific Protein Labeling: Methods and Protocols.* 2014; 8:29-53. [https://doi.org/10.1007/978-1-4939-2272-7\\_3](https://doi.org/10.1007/978-1-4939-2272-7_3)
40. Ugariogu SN, Duru IA, Onwumere FC, Igoli JO. Physicochemical Assessment and Drug Potential of Some Phenylpropanoid and Flavonoid Compounds of Ethyl Acetate Eluate from Umudike Propolis. *Trop. J. Nat. Prod. Res.* 2020; 4(12):1208-1214. <https://doi.org/10.26538/tjnpr/v4i12.30>
41. Olaokun OO, Zubair MS. Antidiabetic activity, molecular docking, and ADMET properties of compounds isolated from bioactive ethyl acetate fraction of *Ficus lutea* leaf extract. *Molecules.* 2023; 28(23):7717. <https://doi.org/10.3390/molecules28237717>
42. Whitty A, Zhong M, Viarengo L, Beglov D, Hall DR, Vajda S. Quantifying the chameleonic properties of macrocycles and other high-molecular-weight drugs. *Drug Disc. Tod.* 2016; 21(5):712-717. <https://doi.org/10.1016/j.drudis.2016.02.005>
43. Jagannathan R. Characterization of drug-like chemical space for cytotoxic marine metabolites using multivariate methods. *ACS omega.* 2019; 4(3):5402-5411. <https://doi.org/10.1021/acsomega.8b01764>
44. Erickson JA, Jalaie M, Robertson DH, Lewis RA, Vieth M. Lessons in molecular recognition: the effects of ligand and protein flexibility on molecular docking accuracy. *J. Med. Chem.* 2004; 47(1):45-55. <https://doi.org/10.1021/jm030209y>
45. Ahmed I, Leach DN, Wohlmuth H, De Voss JJ, Blanchfield JT. Caco-2 cell permeability of flavonoids and saponins from *Gynostemma pentaphyllum*: the immortal herb. *ACS omega.* 2020; 5(34):21561-21569. <https://doi.org/10.1021/acsomega.0c02180>
46. Kirsch V, Bakuradze T, Richling E. Toxicological testing of syringaresinol and enterolignans. *Curr. Res. Tox.* 2020; 1:104-110. <https://doi.org/10.1016/j.crtox.2020.09.002>
47. Bultum LE, Tolossa GB, Kim G, Kwon O, Lee D. *In silico* activity and ADMET profiling of phytochemicals from Ethiopian indigenous aloes using pharmacophore models. *Sci. Rep.* 2022; 12(1):22221. <https://doi.org/10.1038/s41598-022-26446-x>
48. Jung W, Goo S, Hwang T, Lee H, Kim YK, Chae JW, Yun HY, Jung S. Absorption Distribution Metabolism Excretion and Toxicity Property Prediction Utilizing a Pre-Trained Natural Language Processing Model and Its Applications in Early-Stage Drug Development. *Pharm.* 2024; 17(3):382. <https://doi.org/10.3390/ph17030382>
49. Beaumont C, Young GC, Cavalier T, Young MA. Human absorption, distribution, metabolism and excretion properties of drug molecules: a plethora of approaches. *Brit. J. Clin. Pharm.* 2014; 78(6):1185-1200. <https://doi.org/10.1111/bcp.12468>
50. Muehlbacher M, Spitzer GM, Liedl KR, Kornhuber J. Qualitative prediction of blood-brain barrier permeability on a large and refined dataset. *J. Comp.-aided Mol. Des.* 2011; 25:1095-1106. <https://doi.org/10.1007/s10822-011-9478-1>
51. Neumaier F, Zlatopolskiy BD, Neumaier B. Drug penetration into the central nervous system: pharmacokinetic concepts and in vitro model systems. *Pharm.* 2021; 13(10):1542. <https://doi.org/10.3390/pharmaceutics13101542>
52. Wright SH. Molecular and cellular physiology of organic cation transporter 2. *Ame. J. Phys.-Ren. Phys.* 2019; 317(6):F1669-F1679. <https://doi.org/10.1152/ajprenal.00422.2019>
53. Cascaes MM, De Moraes AA, Cruz JN, Franco CD, E Silva RC, Nascimento LD, Ferreira OO, Anjos TO, de Oliveira MS, Guilhon GM, Andrade EH. Phytochemical profile, antioxidant potential, and toxicity evaluation of the essential oils from *Duguetia* and *Xylopi* species (*Annonaceae*) from the Brazilian Amazon. *Antioxidants.* 2022; 11(9):1709. <https://doi.org/10.3390/antiox11091709>
54. Clemen-Pascual LM, Macahig RA, Rojas NR. Comparative toxicity, phytochemistry, and use of 53 Philippine medicinal plants. *Tox. Rep.* 2022; 9:22-35. <https://doi.org/10.1016/j.toxrep.2021.12.002>
55. Durán-Iturbide NA, Díaz-Eufracio BI, Medina-Franco JL. *In silico* ADME/Tox profiling of natural products: A focus on BIOFACQUIM. *ACS omega.* 2020; 5(26):16076-16084. <https://doi.org/10.1021/acsomega.0c01581>
56. Souza HC, Souza MD, Sousa CS, Viana EK, Alves SK, Marques AO, Ribeiro AS, de Sousa do Vale V, Islam MT, de Miranda JA, da Costa Mota M. Molecular Docking and ADME-TOX Profiling of *Moringa oleifera* Constituents against SARS-CoV-2. *Adv. Resp. Med.* 2023; 91(6):464-485. <https://doi.org/10.3390/arm91060035>